CULTURAL HERITAGE

Quantitative Infrared Thermography and Ultrasonic Testing for In-Situ Assessment of Nemrut Dag Stone Statues

AYSE TAVUKCUOGLU (*), EMINE N. CANER-SALTIK (*)

SUMMARY. – *The study was focused on the in-situ non-destructive examination of limestone and sandstone statues in Nemrut Dağ Monument to determine their state of deterioration and the target areas for the application of conservation treatments. The examinations were done by the combined use of quantitative IR thermography (QIRT) and ultrasonic testing supported by the laboratory measurements to obtain standard data from the reference samples. The in-situ QIRT analyses were promising particularly for the detection of detached areas in the forms of scales, stone fragments getting ready to be lost, as well as for the assessment of cracks. The ultrasonic testing allowed soundness assessment of those detached parts and stone surfaces within a crack network. The combined use of those methods was useful to point out the emergency areas that needed conservation treatments and their monitoring.*

1. Introduction

Nemrut Dağ Monument is an archaeological site located in eastern Turkey in the province of Kahta-Adıyaman (Turkey) and positioned at the top of Nemrut Dağ at 2150 m altitude. The site is in the list of World Cultural Heritage since 1987. Here, the mausoleum of the King Antiochus I (69-34 B.C.) is one of the most ambitious constructions of the Hellenistic period. In 62 BC, King Antiochus built a tomb-sanctuary on the mountain top surrounded by huge limestone statues (8-9 m) of himself, two lions, two eagles and various gods. Those statues were once seated, however, the heads of the statues are now scattered throughout the site. There also exist superb reliefs, Lion and Eagle Statues made of sandstone.

(*) Middle East Technical University, Dept. of Architecture, Materials Conservation Laboratory, 06800, Ankara, Turkey; e-mails: aysetavukcuoglu@yahoo.com; canersal@yahoo.com.tr

The study was focused on the in-situ examination of the limestone and sandstone statues in Nemrut Dağ Monument to assess their state of deterioration and to determine the target areas that needed urgent conservation treatments. Such a study necessitated the use of non-destructive investigation methods, such as quantitative infrared thermography (QIRT) together with ultrasonic testing (1-3).

That archaeological site is well-known with its changing and harsh climatic conditions, such as considerable temperature fluctuations in a day, strong winds and heavy precipitation. Due to the inconvenient environmental circumstances of Nemrut Dağ, the care was given to the effective use of those non-destructive methods on site for achieving the data to be processed on quantitative basis and deducing some techniques for their practical use on site for diagnostic and monitoring purposes. The preliminary findings of this study were presented in a conference (4). Here, the completed version of this research is reported in detail.

2. Material and method

The in-situ examination was conducted on the surfaces of the stone statues by using QIRT and ultrasonic testing. Supportive laboratory analyses composed of QIRT and ultrasonic pulse velocity (UPV) measurements were done in order to establish the standard/reference data for better interpretation of in-situ data. For that purpose, sandstone and limestone samples collected from the archaeological site and the stone quarries nearby were examined. The quarry samples cut into 5 cm-thick cubes were artificially weathered by means of salt crystallization cycles according to the RILEM standards (5). The reference data on the sound and deteriorated samples were used for assessing the state of deterioration of the statues on site.

2.1 – *Quantitative IR Thermography*

The surface temperature data obtained by the QIRT survey were used to locate the detached layers or fragments on stone statues at several locations on site and to assess the sound and deteriorated surfaces of the statues in terms of their thermal inertia characteristics. The QIRT survey was done by single and sequential IR imaging of the limestone and sandstone surfaces. The sequential IR imaging was carried out on site by taking infrared images of the target area successively at 10 seconds intervals for a period of 5-10 minutes of heating and cooling periods in daytime. At site, the heating source was the sun while the halogen lamps, providing maximum output of 1000 W, were used to heat up the samples in the laboratory. During the clouds sheltering the sun, the rock body released the heat absorbed from the sun throughout the day. The temperature evolution in time under heating and then cooling exposure conditions

was examined by producing:

1. differential IR images of the target area showing the surface temperature difference between last and first IR images in certain period of time, and
2. the graphs showing temperature difference, ΔT, as a function of square root of time.

The slope of the linear regression obtained by graphs presented the thermal response characteristics of stones as the rates of warming up, R_W, and/or cooling down, R_C. These rates, in fact, are the parameters showing how fast heat can be absorbed or released at the surfaces under the exposure of surrounding conditions. The soundness of the stone surfaces was examined in terms of their R_W and/or R_C rates as well as a comparative value, R, used to compare thermal response characteristics of deteriorated stone surface in relation to the sound stone surface. That ratio was calculated by dividing R_W (or R_C) of the deteriorated/detached area to the R_W (or R_C) of the sound/non-detached area in case that both areas were under the same exposure conditions Eq.[1].

$$R_{RW} = \frac{R_{W-DET}}{R_{W-SOUND}} \quad or \quad R_{RC} = \frac{R_{C-DET}}{R_{C-SOUND}} \tag{1}$$

where R_{RW} is the comparative value of warming up rates (unitless), $R_{W\text{-}DET}$ is the warming up rate of the deteriorated/detached area ($^oC.s^{-1/2}$), $R_{W\text{-}SOUND}$ is the warming up rate of the sound/non-detached area ($^oC.s^{-1/2}$), R_{RC} is the comparative value of cooling down rates (unitless), $R_{C\text{-}DET}$ is the cooling down rate of deteriorated/detached area ($^oC.s^{-1/2}$), $R_{C\text{-}SOUND}$ is the cooling down rate of the sound/non-detached area ($^oC.s^{-1/2}$).

Special care was given to insert the sound and deteriorated stone surfaces into the field of IR image at the same time and to get the effective differential images for the comparison of their thermal responses under the same exposed conditions. The differential IR images of the areas that had more or less flat surfaces and same heating or cooling conditions were used for the examination of thermal response characteristics and degree of deterioration. The interpretation of differential IR images can be misleading in case that the images contain curved edges, shaded and unshaded surfaces together where the sun may warm up the surfaces under investigation differently. The microclimatic conditions affecting the stone surfaces, therefore, were recorded carefully to better-analyse the surface temperature data on quantitative basis. The experimental setups used for data collection at laboratory and on site are shown in Fig. 1.

The IR images were taken with the "ThermoCAM SC640" thermographic equipment. The data on the ambient temperature, relative humidity (RH) and air velocity were recorded by use of an environmental meter, "Kestrel 4000NV" and dataloggers, "HOBOware Pro", while the moisture content in stones were monitored by means of the protimeter, "Surveymaster".

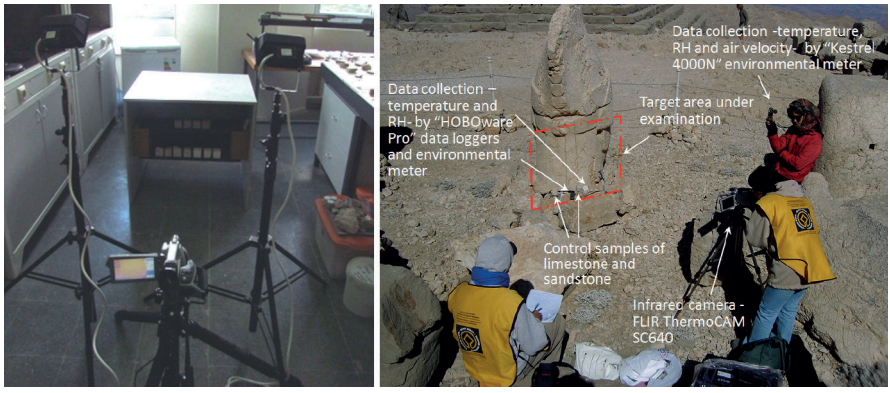


FIG. 1

The experimental setup for thermal monitoring of laboratory samples (at the left) and statues on site (at the right).

2.2 – *Ultrasonic Testing*

The in-situ ultrasonic testing was done in indirect transmission mode (parallel to surface) to estimate the state of deterioration of sound and deteriorated areas. A portable "PUNDIT Plus CNS Farnell" instrument with 220kHz transducers were used both for laboratory and in-situ UPV measurements. The laboratory UPV measurements in direct and indirect transmission modes were taken from three directions of the cubic laboratory samples and the average of three measurements was counted as the UPV_{DIR} and UPV_{IND} values of the laboratory samples. The in-situ UPV measurements were taken from the surfaces of stone statues and the probes were placed on the surfaces of stone statues with a distance of 25 to 40 mm. At least ten readings of transit time were taken on the same position. The soundness assessment of stone surfaces was estimated by comparing their in-situ UPV_{IND} data with the reference UPV data obtained at laboratory taken in direct, UPV_{DIR}, and indirect, UPV_{IND}, transmission modes as well as with the data given in literature (6,7). The Nemrut limestone samples having the UPV_{IND} values below 1250 ms^{-1} were accepted to be severely-deteriorated (6). Due to the anisotropic behaviour of Nemrut sandstones, a special care was given to the direction of bedding layer during the measurements, such as parallel or perpendicular to the bedding layer. The Nemrut sandstones have been classified as "severely-deteriorated", "less-deteriorated" and "sound" according to their UPV_{IND} values below 1000 ms^{-1}, in the range of 1000 ms^{-1} and 2000 ms^{-1}, and above 2000 m^{-1}, respectively (7). The UPV_{IND} data were then evaluated together with the rates of warming up and/or cooling down determined by QIRT analyses. The initial infrared and UPV data taken from untreated stone statues/steles had vital importance for the evaluation of conservation treatments applied on the stone surfaces later on.

3. Results and discussion

The results of the laboratory and in-situ analyses were discussed under respective headings. The analyses were based on the combined interpretation of thermal and ultrasonic data taken on site and at laboratory.

3.1 – *Laboratory analyses*

Here, the relation between the thermal inertia characteristics of the stone samples and their state of deterioration were examined by laboratory analyses. The QIRT and UPV results for the sound limestone and sandstone laboratory samples as well as for the artificially weathered ones by salt crystallisation were summarized in Fig. 2 and Table 1.

The artificially-weathered limestone and sandstone samples presented lower UPV_{DIR} values and faster R_W and R_C than the sound ones (Fig. 2). A good correlation was achieved between the state of deterioration of stone surfaces and their thermal inertia characteristics (Fig. 2). The UPV_{DIR} values of sound and deteriorated limestone and sandstone samples were found to present strong correlation with their warming up rates, with the squared correlation coefficient of 0.98 for limestone and 0.96 for sandstone samples. The relationship between the warming up rates and their UPV_{IND} values, especially for the sandstones taken parallel to the bedding layer, designated good correlation with the squared correlation coefficient of 0.85 for sandstone and 0.55 for limestone samples. The data meant that any failure changing the state of preservation of the stone surface was expected to affect its thermal response to the exposed conditions.

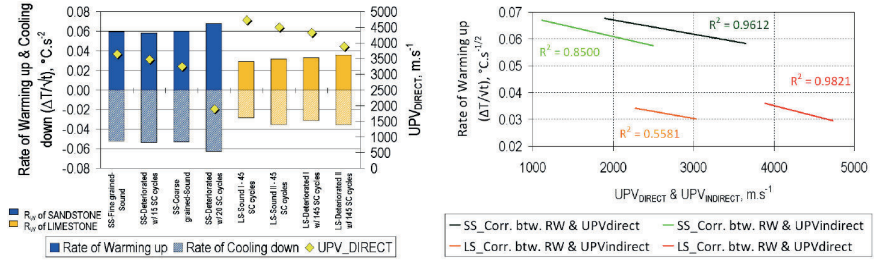


FIG. 2

The UPV_{DIR}, R_W and R_C values of sound and artificially-weathered sandstone (SS) and limestone (LS) samples (at the left) and the good correlation between the UPV values of those samples taken in direct and indirect transmission modes and their R_W (at the right).

The limestone samples had higher UPV values and slower R_W than the sandstone samples due to their higher thermal inertia characteristics (Fig. 2, Table 1 and Table 2). The sound limestone sample were determined to have UPV_{DIR},

UPV_{IND}, R_W and R_C values of 4615m.s^{-1}, 3140m.s^{-1}, 0.0304ºC.s$^{1/2}$, 0.0319ºC.s$^{1/2}$, respectively, while the sound fine-grain sandstone sample having the values 3648m.s^{-1}, 2497m.s^{-1}, 0.0583ºC.s$^{1/2}$, and -0.0520ºC.s$^{1/2}$, respectively. The sound coarse grain sandstone sample presented similar values to the fine-grain one with the UPV_{DIR}, UPV_{IND}, R_W and R_C values of 3253m.s^{-1}, 1974m.s^{-1}, 0.0600ºC.s$^{1/2}$, -0.0533ºC.s$^{1/2}$, respectively. The UPV_{IND} values of limestone and fine-grain sandstone samples were 0.68 times less than their UPV_{DIR} values while coarse grain sandstone sample presented slightly less UPV_{IND} values, with ratio of 0.60, when compared to its UPV_{DIR} value.

The deteriorated stone samples presented lower UPV values and faster warming up and cooling down rates than the sound ones. In other words, the reduction in physico-mechanical properties decreased the thermal inertia characteristics of the deteriorated stone samples. The results for the sandstone and limestone samples were summarized in Table 1 and Table 2.

Table 1

The results of the laboratory analyses on reference stone samples in terms of UPV_{DIR} and UPV_{IND} values as well as the ratio showing the reduction in UPV values of deteriorated samples in comparison to the sound one.

Samples	$UPV_{DIR\text{-}SOUND}$	$UPV_{DIR\text{-}DET}$	$UPV_{IND\text{-}SOUND}$	$UPV_{IND\text{-}DET}$	$\frac{UPV_{DIR\text{-}DET}}{UPV_{DIR\text{-}SOUND}}$	$\frac{UPV_{IND\text{-}DET}}{UPV_{IND\text{-}SOUND}}$
	m.s^{-1}	m.s^{-1}	m.s^{-1}	m.s^{-1}	unitless	unitless
Limestone-I	4615	4330	3140	3127	0.94	0.78
Limestone-II	4615	3886	3140	2415	0.84	0.77
Sandstone-I	3648	3479	2497	2126	0.95	0.85
Sandstone-II	3648	1891	2497	1113	0.52	0.45
The deteriorated limestones were artificially weathered with 145 cycles and the deteriorated sandstones were artificially weathered with 15 and 20 cycles of salt crystallization, respectively.						

Table 2

The results of the laboratory analyses on reference stone samples in terms of R_W, R_C, and comparative values of R_{RW} and R_{RC}

Samples	$R_{W\text{-}SOUND}$	$R_{W\text{-}DET}$	$R_{C\text{-}SOUND}$	$R_{C\text{-}DET}$	R_{RW}	R_{RC}
	ºC.s$^{-1/2}$	ºC.s$^{-1/2}$	ºC.s$^{-1/2}$	ºC.s$^{-1/2}$	unitless	unitless
Limestone-I	0.0304	0.0329	-0.0319	-0.0331	1.131	1.095
Limestone-II	0.0304	0.0357	-0.0319	-0.0352	1.227	1.244
Sandstone-I	0.0583	0.0594	-0.0520	-0.0534	1.019	1.027
Sandstone-II	0.0583	0.0679	-0.0520	-0.0625	1.165	1.202
The R_W and R_C values of the sound and artificially weathered stone samples were calculated for the initial 120s of heating and cooling periods at boundary conditions of 19ºC and 40% RH.						

The sandstone sample artificially weathered with 15 cycles of salt crystallization seemed to have still enough strength while the ones weathered with 20 or more cycles presented noticeable reduction in their UPV values. The UPV_{DIR} and UPV_{IND} values of deteriorated samples decreased to 1891 $m.s^{-1}$ and 1113 $m.s^{-1}$, respectively, while their R_W and R_C values increased to 0.0679ºC.$s^{1/2}$ and -0.0625ºC.$s^{1/2}$. The reduction of 50% in physico-mechanical properties corresponded to 1.17-1.20 times faster warming up or cooling down in deteriorated sandstone samples.

The limestone samples artificially weathered with 145 cycles of salt crystallization seemed to still have enough strength with the UPV_{DIR} and UPV_{IND} values of 3886$m.s^{-1}$ and 2415$m.s^{-1}$, respectively. The reduction of 15% in physico-mechanical properties corresponded to 1.23-1.24 times faster warming up or cooling down in deteriorated limestone samples.

Due to the higher thermal inertia characteristics of Nemrut limestone, the surface temperature change under the exposed conditions seemed to occur in small ranges when compared with the higher thermal response characteristics of Nemrut sandstones. However, the QIRT analyses on limestone samples presented higher sensitivity in relation to the physico-mechanical properties when compared with the analyses on sandstone samples. This might be due to the anisotropic behaviour of sandstone and further studies are needed to investigate the relation between the direction of bedding layer and thermal inertia and physico-mechanical properties.

3.2 – *In-situ analyses*

Some in-situ case studies are presented here: the Antiochus Head at the east terrace (Fig. 3), the sandstone stele at the north terrace (see Fig. 4 and Table 3), the limestone Kommagene Head at the west terrace (see Fig. 5, Fig. 6 and Table 4). Those case studies were the examples for the joint interpretation of the in-situ QIRT and UPV data and laboratory data.

The detachments in the form of scales and/or fragmental disintegration are the emergency areas where some treatments are needed to be done. Those separating areas and their extent were detected in differential IR images easily due to their low thermal inertia characteristics while they could not be observed visually. For instance, at the north side of Antiochus Head at the east terrace, the very emergency area was determined where there were deep cracks crossing each other (Fig. 3). That area warmed up and cooled down the fastest among the neighbouring non-detached surfaces. The differential IR images produced for that region signalled the completely detached stone fragment under the very risk of material loss.

The edges of detached scales on the sandstone stele at the north terrace could be noticed visually while their extent in the rock body could not be observed visually (Fig. 4). The sound sandstone rock body, if each bedding layer is still in good adhesion with each other, present a high thermal inertia characteristics in differential IR images with the least temperature change and slower rates of warming up and cooling down than the detached layers. The detaching

scales, on the other hand, were observed to have warmer surfaces than the non-detached areas in individual IR images during the heating period and warmed up and cooled down faster than the non-detached surfaces. The state of deterioration of those detaching scales was assessed in terms of UPV_{IND} and R_W. The joint interpretation of differential IR images and UPV_{IND} and R_W data has shown that some detaching scales were found to be severely deteriorated due to the UPV_{IND} values below 1000ms^{-1} while some detaching scales were found to be still sound (Table 4). The detached scales presented R_W about 1.2 times faster than the non-detached surfaces while the severely-deteriorated parts of those detached layers were determined to warm up 1.5-1.9 times faster than the non-detached sandstone surfaces (Table 3). The surface of the non-detached area in Zone 3 was determined to be severely-deteriorated due to its UPV value below 1000m.s^{-1} (see AR05 in Table 3). This meant that the R_{RW} of the detached areas in Zone 3 should be expected to present larger values if the reference R_W value could be achieved for the sound/non-detached surface.

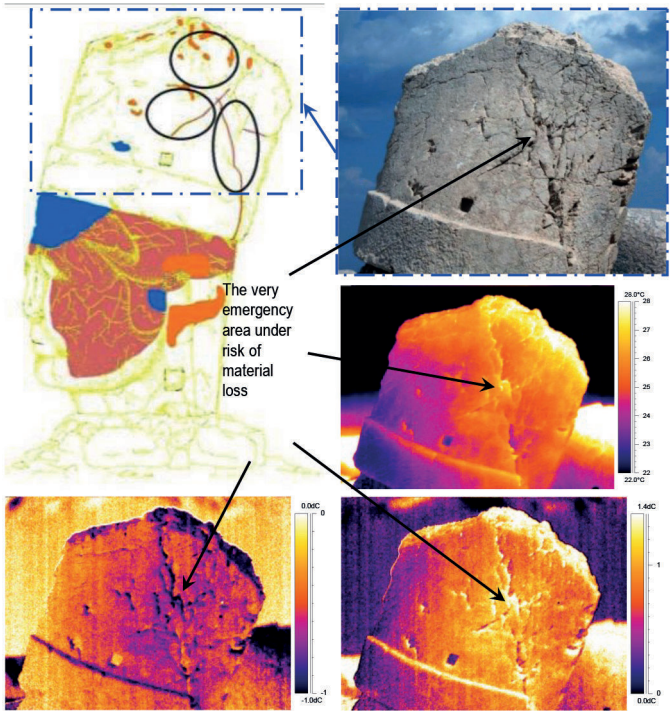


FIG. 3

The map showing the distribution of weathering forms the Antiochus Head (north side) at the east terrace (at the left top), the digital photo of the area under QIRT examination (at the right top), and the IR image of the selected area at the climatic conditions of 23.7ºC and 38% (at the right middle), its differential images processed for the cooling period of 60 s (at the left bottom) and heating period of 241 s (at the right bottom).

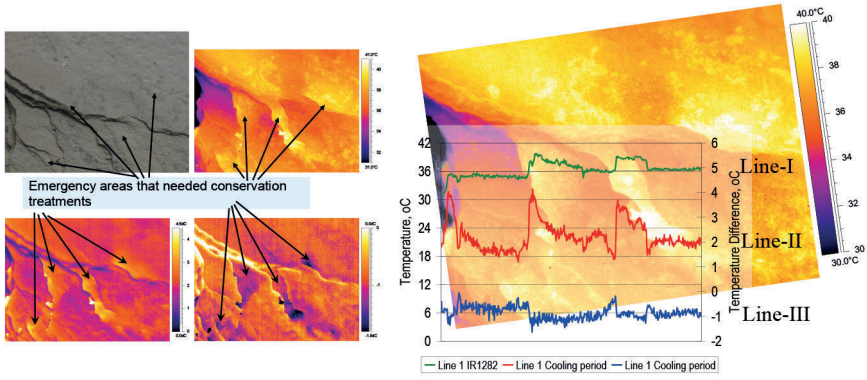


FIG. 4

Partial view of the sandstone stele at the north terrace and its IR image taken at the climatic conditions of 22.8ºC and 40%RH (at the left top); the differential IR images processed for the heating period of 240s and for the cooling period of 121s, respectively (at the left bottom); Line-I (in green) showed the surface temperature through the layers of three bedding layer as positioned on the individual IR image while Line-II (in red) and Line-III (in blue) showed the temperature difference during the heating and cooling periods, respectively, through the path of the Line-I.

Table 3

The rate of warming up of the detached and non-detached surfaces, R_W, the comparative value for the detached surfaces, R_{RW}, and the $UPV_{IND}(7)$ data for the surfaces of the sandstone stele at the north terrace. (The R_W data was obtained at the climatic conditions of 6.6 ºC and 75% RH during the heating period of 1368s).

Sandstone		UPV_{IND} (7)	R_W	R_{RW}
Zone	**Sample Area**	**$m.s^{-1}$**	**$ºC.s^{-1/2}$**	**Unitless**
1	AR20-non-detached	1265	0.0414	1.000
	AR27-non-detached	NA	0.0462	1.116
	AR12-detached	885	0.0620	1.498
	AR28-detached	885	0.0639	1.544
	AR13-detached	885	0.0668	1.614
2	AR11-non-detached	1067	0.0394	1.000
	AR10-non-detached	NA	0.0426	1.081
	AR06-detached	NA	0.0714	1.812
	AR07-detached	596	0.0750	1.904
3	AR05-non-detached	939	0.0424	1.000
	AR03-detached	1138	0.0535	1.259
	AR04-detached	1050	0.0574	1.351
4	AR02-non-detached	1301	0.0339	1.000
	AR01-non-detached	1798	0.0403	1.189
	AR023-detached	NA	0.0565	1.667
	AR024-detached	NA	0.0570	1.681

The deep cracks let water leakages to the deeper layers and the fragmental disintegration were mostly associated with the deeper cracks. The pattern of deep cracks, therefore, showed the emergency areas getting ready to be lost by fragmental disintegration. On the Kommagene Head made of limestone, the crack pattern including the visible and invisible cracks and the deteriorated parts due to the fragmental disintegration could be observed in the individual and differential IR images (Fig. 5).

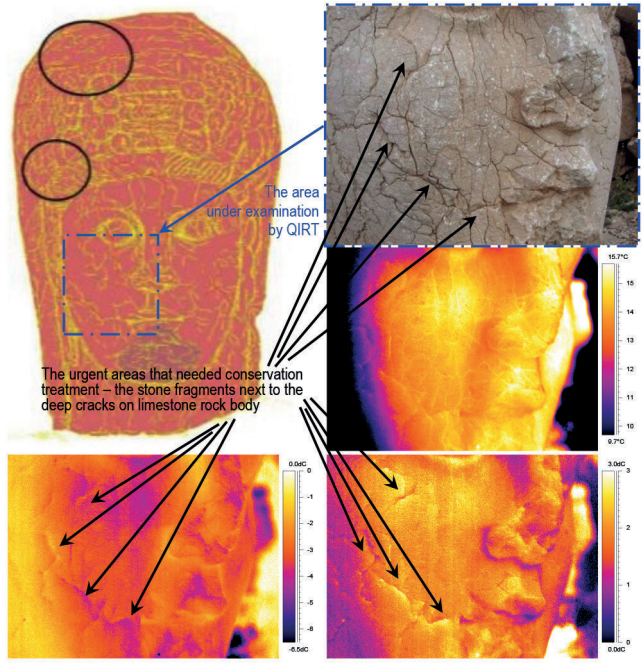


FIG. 5

The map showing the distribution of weathering forms on the Kommagene Head at the west terrace -microkarstification in red and pitting in yellow- (at the left top);the digital photo of the area under QIRT examination (at the right top); the IR image of the selected area at the climatic conditions of 10.1°C and 62% (at the right middle), its differential images processed for the cooling period of 1112s and heating period of 634s, respectively (at the bottom).

However, the deeper and superficial cracks could not be well-distinguished in the individual IR images. The investigation of deeper cracks in the differential images needed to achieve longer temperature differences during heating and cooling. Since sufficient heating and cooling conditions were achieved on site, the pattern of deeper cracks on the left cheek of Kommagene and the emergency areas having the risk of material loss due to the fragmental disintegration were visible clearly in the differential images with larger temperature range (Fig. 5). The superficial cracks were visible in differential images only in low temperature ranges

belonging to the earlier stages of cooling (Fig. 7). They disappeared in differential images with larger temperature range. The detaching stone fragments from the rock body that could not be observed visually were also visible in differential IR images due to their faster warming up and cooling down when compared with the non-detached rock surfaces. The soundness of those critical zones was examined in terms of UPV_{IND} and R_W. The joint interpretation of differential IR images and UPV_{IND} and R_W data has shown that the stone fragments separating from the rock body were still sound due to the UPV_{IND} values above 1250ms^{-1} (Fig. 6 and Table 4). The separating limestone fragments were determined to warm up 1.2-1.4 times faster than the non-detached surfaces (Table 4).

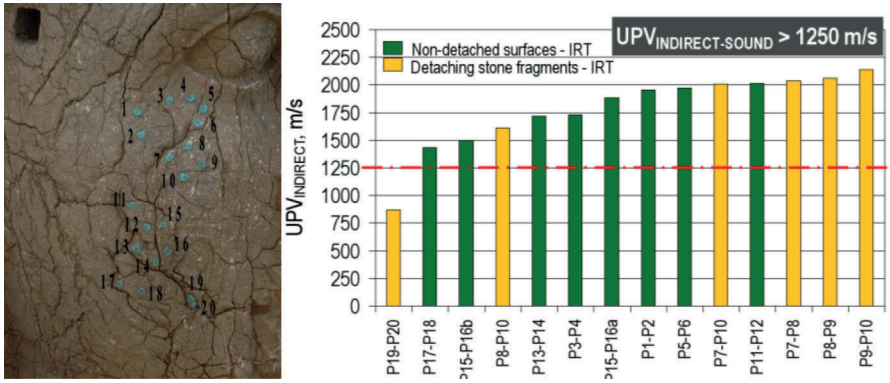


FIG. 6

Partial view of Kommagene Head at the west terrace showing the locations where UPV_{IND} measurements were taken (at the left) and the chart showing the UPV_{IND} values for the non-detached sound surfaces and detaching stone fragments.

Table 4

The rate of warming up of the detaching stone fragments and non-detached sound surfaces, R_W, the comparative value for the detaching fragments, R_{RW}, and the UPV_{IND} values for the limestone surfaces of Kommagene Head at the west terrace. (The IR image of the examined area were taken at the climatic conditions of 10.1°C and 62%RH during the heating period of 634s).

Limestone	UPV_{IND}	R_W	R_{RW}
Sample Area		**°C.s$^{-1/2}$**	**unitless**
AR03-non-detached	1729	0.0775	1.000
AR14-non-detached	1970	0.0811	1.047
AR15-non-detached	1955	0.0929	1.199
AR16-detached	2060	0.0961	1.240
AR01-detached	NA	0.106	1.368
AR02-detached	2039	0.1043	1.346

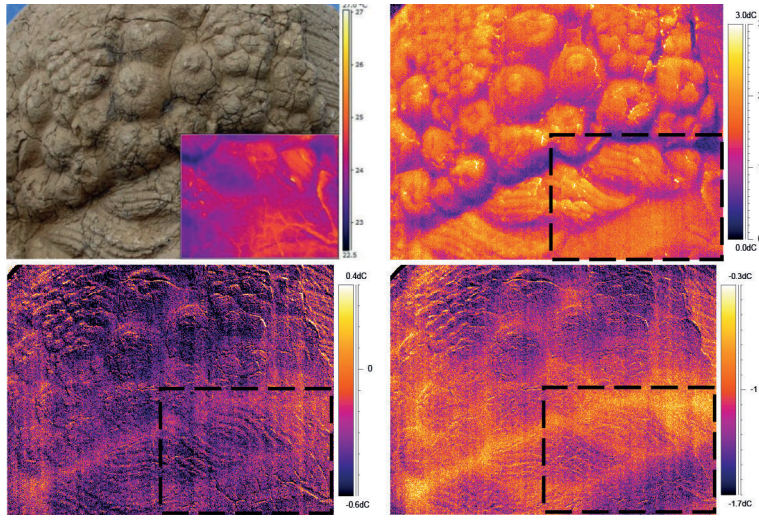


FIG. 7

Partial view from north side of Kommagene Head at the west terrace and its IR image taken at the climatic conditions of 21.6°C and 32% RH, designating the pattern of superficial cracks at the forehead with warmer lines (at the left top); the differential images processed for the heating period of 272s (at the right top), for the earlier period of cooling (at the left bottom) and for the cooling period of 1072s with larger temperature range (at the right bottom).

4. Conclusion

The in-situ QIRT analyses were found to be promising particularly for the detection of detachments areas and their extent, assessment of cracks and monitoring of conservation treatments. The in-situ UPV measurements that could only be done in indirect transmission mode, allowed assessing the state of deterioration for the detached parts on quantitative basis.

The use of QIRT and ultrasonic testing on site complemented each other to point out the emergency areas that needed conservation treatments. Those emergency areas had priority for the conservation treatments, such as for the deep cracks to be treated against water penetration, the prevention of losses due to scales or fragmental disintegration and control of decay/detaching mechanisms in the rock body. The success of the conservation treatments seemed to be controlled in-situ by collaborative use QIRT and ultrasonic testing, especially with the parameters, UPV_{IND}, R_{RW} and R_{RC}. The establishment of in-situ reference data for the sound and non-detached surfaces has vital importance for the calculation of R_{RW} and R_{RC} values. A special care, therefore, should be given to the soundness assessment of reference area that will increase the accuracy of in-situ QIRT analyses.

The further studies at Nemrut Dag archaeological site will include the long-term monitoring and conservation studies. The next stage of the conservation project, therefore, involves the training activities on QIRT and ultrasonic testing for the researchers of the region. For the training activities, the results of the study have a guiding feature that present the methods for in-situ testing procedures and the data analyses conducted Nemrut Dag stone monuments on site. The reference data obtained from the control samples at laboratory and the in-situ data obtained from the emergency areas of limestone and sandstone statues/steles before treatment established the fundamental data for the in-situ soundness assessment and monitoring studies after treatment.

Acknowledgement

The authors would like to express their gratitude to Dr. Ermanno Grinzato who was the strategic partner of the "*Monumentslab - 206710"* EU Project for the improvement of NDT research capacity of METU-MCL (Materials Conservation Laboratory) and gratefully thank for his scientific guidance, remarkable contributions and constant encouragement throughout this project. The authors will always remember him with respect and love for his efforts, particularly on the improvement of in-situ QIRT analyses in the field of cultural heritage conservation.

The authors would also like to acknowledge the project METU AGÜDOS 06.02.01.2.00.11 "Commagene Nemrut Conservation Development Programme", supported by the Ministry of Tourism and Culture-Turkey.

REFERENCES

(1) E. Grinzato, S. Marinetti, P.G. Bison, M. Concas, *Comparison of ultrasonic velocity and IR thermography for the characterisation of stone,* J. of Infrared Phys. and Techn., **46**, 63-68, 2004.

(2) E. Grinzato, G. Cadelano, P.Bison, A. Petracca, *Seismic risk evaluation aided by IR thermography,* Proc. SPIE, **7299**, *Thermosense XXXI*, Burleigh D.D. and Dinwiddie R.B. (Eds), (Orlando, USA, 2009).

(3) A. Tavukçuoğlu, S. Akevren, E. Grinzato, *In-situ examination of structural cracks at historic masonry structures by quantitative infrared thermography and ultrasonic testing*, J. of Modern Optics, **57**(18), 1779-1789*,* 2010.

(4) A. Tavukçuoğlu, E.N. Caner-Saltik, K.G. Akoğlu, M. Isikoğlu, E. Caner, *In-situ examination of Nemrut Dağ sandstone and limestone statues by NDT methods*, Proc. of Intern. Conf. on *Jardins De Pierrres. Conservation of stone in Parks, Gardens and Cemeteries*, (Paris, France, 22-24 June 2011 (pp. 204-213) (France: SFIIC, Institut National du Patrimoine, 2011).

(5) RILEM, *Tentative Recommendations, Commission 25, PEM, Recommended tests to measure the deterioration of stone and to assess the effectiveness of treatment methods*, Materiaux and Construction, **13**, 173-253, 1980.

(6) E. Caner, *Limestone decay in historic monuments and consolidation with nanodispersive calcium hydroxide solutions,* (Unpublished Ph.D. Thesis, Graduate Program in Restoration, Dept. of Architecture, Middle East Techn. Univ., Ankara, Turkey, 2011).

(7) K.G. Akoğlu, *Deterioration of Nemrut sandstone and development of its conservation treatment,* (Unpublished Ph.D. Thesis, Graduate Program in Restoration, Dept. of Architecture, Middle East Techn. Univ., Ankara, Turkey, 2011).

INDEX

Advanced technologies

U. GALIETTI, D. PALUMBO, R. DE FINIS, F. ANCONA, *Fatigue damage evaluation with new thermal methods* Pag. 387

M.N. LITVINOVA, V. KRISHTOP, N. KIREEVA, Y. PONOMARCHUK, *Conversion of incoherent IR-radiation into visible radiation in nonlinear crystals* » 405

A. LIBBRA, A. MUSCIO, *Reverse use of an infrared emissometer for measurement of thermal conductivity* » 413

Bio applications

I. BENKO, *Histographic method as a tool of thermal image processing* » 423

V. REDAELLI, G. PIZZAMIGLIO, P. SELLERI, N. DI GIROLAMO, P.A. MARTINO, F. LUZI, *Environmental assessment of terrarium in the main species of reptiles through the thermography technique. Preliminary results* » 433

Buildings and infrastructures

A. BORTOLIN, G. FERRARINI, P. BISON, G. CADELANO, *Thermal performance measurement of the building envelope by infrared thermography* » 441

E.C. ROBISON, C. ESATRADA, *The application of Infrared Thermography to Condition Assessments of Guastavino Vaulting* » 447

G. FERRARINI, P. BISON, A. BORTOLIN, G. CADELANO, M. GIROTTO, U. NAZZALI, F. PERON, M. VOLINIA, *Energy survey of a historical building by infrared thermography* » 453

Cultural heritage

A. TAVUKCUOGLU, *Quantative Infrared Thermography and Ultrasonic Testing for In-Situ Assessment of Nemrut Dag Stone Statues* » 459

Image and data analysis

W. SWIDERSKI, D. NESTERUK, V. VAVILOV, D. DERUSOVA, *Data Fusion in IR Thermographic Detection of Landmines and NDT of Composites* » 473

A.A.S. MOHAMMED, S.M. HAMEED, *A Development Formula to Evaluate the Band Width of an Image for a digital Camera* » 479

Industrial applications

A. KHALIFA, M. MARCHETTI, L. IBOS, V. FEUILLET, J. DUMOULIN, M. BUÈS, L. BOUILLOUD, *Monitoring of traffic incidence on pavement surface temperature* » 487

Nondestructive evaluation

L. VEGA, P. VENEGAS, I. SAEZ DE OCARIZ, M. VANDEWAL, A. BROOK, E. CRISTOFANI, P. MOUNAIX, J.P. GUILLET, S. WOHNSIEDLER, C. MATHEIS, F. OSPALD, *Validation of a Novel NDT Technique with Infrared Thermography* » 493

P. VENEGAS, L. VEGA, J. GUEREDIAGA, I. SAEZ DE OCARIZ, *Instrumentation Technology based on Infrared Thermography for the Control of Aeronautical Composite Components Subjected to Certification Load Tests* » 499

A. ELHASSNAOUI, S. BELATTAR, S. SAHNOUN, *Determination of defects thermal effusivities by pulsed thermography* » 505

Sensors

W. ALLASIA, P. PRINETTO, A. RIVA, *EAGLE, a compact vision system with two simultaneous field of view* » 513